Synthesis, structure, and magnetic properties of $Pr_5Co_{19}B_6$

Yi Chen, X. Li, and L. Chen
Institute of Physics and Center for Condensed Matter Physics, Chinese Academy of Sciences, Beijing 100080, People's Republic of China

J. K. Liang
International Center for Materials Physics, Chinese Academy of Sciences, Shenyang 110015, People's Republic of China

B. G. Shen
State Key Laboratory of Magnetism, Institute of Physics, Chinese Academy of Sciences, Beijing 100080, People's Republic of China

Q. L. Liu
Institute of Physics and Center for Condensed Matter Physics, Chinese Academy of Sciences, Beijing 100080, People's Republic of China
(Received 11 January 1999; revised manuscript received 24 May 1999)

A compound $Pr_5Co_{19}B_6$ has been synthesized successfully and its crystal structure has been investigated by x-ray powder diffraction. It belongs to the $R_{m+n}Co_{5m+3n}B_{2n}$ (R=rare earth) family with $m=2$ and $n=3$. The space group is $P6/mmm$. The lattice parameters are $a=5.1264(4)$ Å and $c=16.5602(6)$ Å. Each unit cell contains one formula unit of $Pr_5Co_{19}B_6$, and there are nine kinds of equivalent positions in each unit cell, i.e., $1b$, $2e(1)$, $2e(2)$, $4h(1)$, $6i(1)$, $6i(2)$, $3f$, $2d$, and $4h(2)$, which are occupied by $1Pr^{(1)}$, $2Pr^{(2)}$, $2Pr^{(3)}$, $4Co^{(1)}$, $6Co^{(2)}$, $6Co^{(3)}$, $3Co^{(4)}$, $2B^{(1)}$, and $4B^{(2)}$, respectively. Magnetic measurements indicate that this compound is ferromagnetic with a Curie temperature of 380 K. Its saturation magnetic moment at 5 K and room temperature are $23.7\mu_B$/f.u. and $11.9\mu_B$/f.u., respectively. Based on the experimental results of the saturation magnetization, three kinds of Co sites with different magnetic moment are proposed. The $Pr_5Co_{19}B_6$ compound exhibits huge planar anisotropy with an anisotropy field of 250 kOe at 5 K. No spin reorientation was detected from the temperature dependence of the magnetization and the temperature dependence of the ac susceptibility curves from 5 K to room temperature. The behavior of magnetocrystalline anisotropy is analyzed using the single-ion model.

I. INTRODUCTION

In the ternary systems R-T-B (R=rare earth, T=Co or Fe) there exist many compounds, some of which are outstanding candidates for the production of permanent magnets. This is in particular true for the compounds $Nd_2Fe_{14}B$.[1] In the case of R-Co-B systems, it has been shown that[2] a homologous series of compounds exists between the compositions RCo_5 and RCo_3B_2. This series is represented by a general formula $R_{1+n}Co_{5+3n}B_{2n}$, which is formed by alternating stacking of one layer RCo_5 and n layers RCo_3B_2 along the c axis. Huge magnetic anisotropy is found in the $Sm_{1+n}Co_{5+3n}B_{2n}$ system. For example, the anisotropy fields of $SmCo_5$, $SmCo_4B$, $Sm_3Co_{11}B_4$, $SmCo_3B_2$ are found to be 710, 1200, 1160, 1300 kOe at 4.2 K, respectively.[3] The strength of the individual contributions of the Co sites to the magnetic anisotropy and the magnetic moments of the nonequivalent Co sites in these compounds have been studied using nuclear magnetic resonance[4] (NMR) and neutron diffraction.[5] Smit, Thiel, and Buschow[6] determined the crystal-field parameters by measuring the Mössbauer spectrum of $Gd_{1+n}Co_{5+3n}B_{2n}$. It was shown that B substitution for Co entails an increase in the second-order crystal-field parameters, which brings about the enhancement of the magnetocrystalline anisotropy. However, the Curie temperature (T_C) and saturation moment (M_S) of these $R_{1+n}Co_{5+3n}B_{2n}$ intermetallics are too low to be suitable for permanent magnet fabrication.[7–9] In order to overcome these drawbacks, many investigations[10–14] have been focused on either substituting Co by Fe or preparing materials with additional atoms located interstitially by gas-solid reaction modifications. Here, we demonstrate an alternative strategy, in which we propose a similar series $R_{m+1}Co_{5m+3}B_2$ with high Co content. This series, crystallographically equivalent to $R_{1+n}Co_{5+3n}B_{2n}$, is expected to consist of m layers RCo_5 and one layer RCo_3B_2. After we carefully investigated the phase diagrams of R-Co-B (R=Pr, Nd, Sm, Gd) systems at relatively low temperatures, the series $R_{m+1}Co_{5m+3}B_2$ with $m=2$ was confirmed to exist.[15,16]

In fact, the two homologous series mentioned above can be expressed by a general formula $R_{m+n}T_{5m+3n}B_{2n}$ which is formed by alternative stacking m parts RT_5 with n parts RT_3B_2.[17] Some of the compositions represented by this formula can be regarded as real compound compositions, and we can presume that $R_{m+n}Co_{5m+3n}B_{2n}$ have high T_C and M_S due to the high Co content. Such compounds are not known in the R-Co-B system, but we suppose that $R_{m+n}Co_{5m+3n}B_{2n}$ intermetallics may be obtained by annealing the samples at relatively low temperature for several months. In this paper, we report the experimental results of $Pr_5Co_{19}B_6$ ($m=2$ and $n=3$) on the synthesis, crystal structure and its magnetic properties as well.

II. EXPERIMENT

The samples examined in this work were prepared by melting raw materials of more than 99.9% purity in an arc furnace. In order to avoid the loss of boron during melting, boron was added through a master alloy of CoB. To ensure

the homogeneity of the samples, the ingots were turned and melted several times. The weight loss of the samples during melting was less than 1%. After arc melting, the samples were wrapped in Ta foil and sealed in a quartz tube. The samples were annealed in vacuum at 873 K for two months and then rapidly cooled to room temperature. The phase identification of the samples was carried out by x-ray powder diffraction, using a four-layer monochromatic focusing Guinier de Wolff camera with Co K_α radiation. The x-ray-diffraction (XRD) data, used to determine the crystal structure parameters, were obtained in a Rigaku Rint diffractometer with Cu K_α radiation with graphite-monochromator, operating in a step-scan mode with a scanning step of $2\theta = 0.02°$ and a sampling time of 2 s. The XRD pattern of a sample consisting of powder particles ($\leqslant 40$ μm), which were magnetically aligned at room temperature, was used to determine the easy magnetization direction in this compound. Measurement of the ac susceptibility of the bulk sample was performed between 5 K and room temperature with a frequency of 314 Hz. Since the investigated compound exhibits planar anisotropy at room temperature, the magnetic alignment was carried out by means of the rotation-alignment technique. In this technique, the fine-powdered particles are mixed with epoxy resin and embedded in a Teflon tube of cylindrical shape. The tube was mounted on a motor which rotates the tube around its axis in a perpendicular magnetic field of about 1.0 T until the epoxy resin solidifies. It is easily understood that the cylinder axis of the aligned samples, being identical to the rotation axis during the magnetic-alignment procedure, is the hard magnetization direction of the compounds with planar anisotropy. The magnetic properties of the sample were determined in a magnetic balance, a vibrating-sample magnetometer and a superconducting quantum interference device (SQUID).

III. RESULTS AND DISCUSSION

A. Crystal structure of the compound $Pr_5Co_{19}B_6$

The $Pr_5Co_{19}B_6$ phase is normally not found in as-cast alloys, owing to the fact that it results from a peritectoid reaction below 800 °C. The reaction is essentially $2PrCo_4B + Pr_3Co_{11}B_4 \leftrightarrow Pr_5Co_{19}B_6$. It generally needs prolonged annealing of several weeks at a temperature below 800 °C. Figure 1 shows the XRD pattern for the sample annealed at 600 °C for two months. The XRD pattern can be successfully indexed with a hexagonal cell with lattice parameters $a = 5.1264(4)$ Å and $c = 16.5602(6)$ Å.[18,19] The unit-cell volume is 376.88(4) Å^3 and the calculated density is $D_x = 8.32$ g/cm^3. An initial structure model was derived from the isostructural $Lu_5Ni_{19}B_6$ based on the space group $P6/mmm$. There is one $Pr_5Co_{19}B_6$ formula unit in the cell: the Pr atoms occupy three different crystallographic sites ($1b, 2e_1, 2e_2$), the Co atoms four different positions ($4h_1, 6i_1, 6i_2, 3f$), and B the $2d$ and $4h_2$ positions. Rietveld refinement[20–22] was performed and the final refinement results are shown in Fig. 1 and Table I. Table II lists the selected atom distances in this compound. The pattern factor R_P, the weighted pattern factor R_W, and the expected pattern factor $R_{\rm exp}$ are 9.6%, 12.3%, and 6.1%, respectively. Finally, the crystal structure of $Pr_5Co_{19}B_6$ is illustrated in Fig. 2.

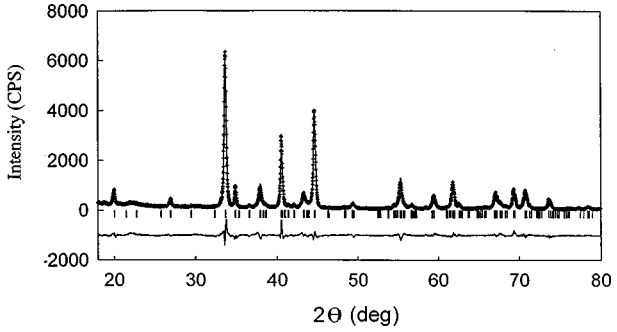

FIG. 1. Rietveld analysis of the XRD pattern of $Pr_5Co_{19}B_6$. The experimental data are indicated by crosses and the calculated profile by the continuous line overlaying them. The lower curve is the difference between the experimental and calculated intensity at each step, plotted on the same scale and shifted a little downwards for clarity.

B. Curie temperature and exchange interactions

Figure 3 shows the temperature dependence of the magnetization $M(T)$ for a free powder sample of $Pr_5Co_{19}B_6$ in a low field of 0.05 T measured in the SQUID in the temperature range below room temperature and in a vibrating sample magnetometer above room temperature. A Curie temperature (T_C) of 380 K was determined from M^2-T plots by extrapolating M^2 to zero. The Curie temperature of $Pr_5Co_{19}B_6$ is determined by three different exchange-coupling constants: J_{TT}, J_{RT}, and J_{RR}. The *R*-*R* interaction is generally neglected because it is much smaller than the *T*-*T* and the *R*-*T* interaction. In addition, there are few *R*-*R* bonds in the Co-rich compounds. The $3d$-$4f$ interaction J_{RT} has only a minor influence on the Curie temperature. However, it dominates the molecular field experienced by the *R* moment that, in turn, determines the temperature dependence of the magnetic moment and the magnetocrystalline anisotropy of the *R* ions. Since the Co-Co exchange-coupling constant is one order of magnitude larger than the *R*-Co exchange-coupling constant, the Curie temperature T_C of $Pr_5Co_{19}B_6$ is mainly determined by the Co-Co interaction. Thus the Curie temperature T_C of $Pr_5Co_{19}B_6$ is

$$T_C = \{T_{\rm PrPr} + T_{\rm CoCo} + [(T_{\rm CoCo} - T_{\rm PrPr})^2 + 4T_{\rm PrCo}]^{1/2}\}/2, \tag{1}$$

where T_{ii} ($i = {\rm Pr}, {\rm Co}$) and $T_{\rm PrCo}$ can be written as

$$T_{ii} = (2A_{ii}Z_{ii}G_i)/(3k_B) \tag{2}$$

and

$$T_{\rm PrCo} = [2A_{\rm PrCo}(Z_{\rm PrCo}Z_{\rm CoPr}G_{\rm Pr}G_{\rm Co})]^{1/2}, \tag{3}$$

where $G_i = (g_i - 1)^2 J_i(J_i + 1)$, Z_{ij} is the number of nearest j atom neighbor of an i atom, g_i is the Lande factor of the i atom. Substitution of B at $2c$ and $4h_2$ sites for Co leads to the decrease of Co-Co exchange interaction. Thus both the magnetic dilution and the decrease of Co-Co exchange interaction result in a drastic decrease of T_C compared with the parent compound $PrCo_5$.

TABLE I. Atomic positions and lattice parameters of the $Pr_5Co_{19}B_6$ structure obtained from the powder x-ray-diffraction pattern refinement according to the $P6/mmm$ space group.

Atom	Position	x/a	y/b	z/c	B (Å^2)	Number of neighbor atoms
Pr(1)	$1b$	0	0	0.5000	0.10	12Co(1)+6B(1)+2Pr(2)
Pr(2)	$2e_2$	0	0	0.2951(3)	0.10	6Co(1)+6Co(2)+6Co(3) +Pr(1)+Pr(3)
Pr(3)	$2e_1$	0	0	0.0955(2)	0.37	6Co(3)+6Co(4)+6B(2) +Pr(3)+Pr(2)
Co(1)	$6i_2$	0.5000	0	0.4149(2)	0.77	2Pr(1)+2Pr(2)+4Co(1) +2Co(2)+2B(1)
Co(2)	$4h_1$	0.3333	0.6667	0.2943(6)	0.95	3Pr(2)+3Co(1) +3Co(2)+3Co(3)
Co(3)	$6i_1$	0.5000	0	0.1745(3)	0.18	2Pr(2)+2Pr(3)+2Co(2) +4Co(3)+2B(2)
Co(4)	$3f$	0.5000	0	0.0000	0.29	4Pr(3)+4Co(4)+4b(2)
B(1)	$2d$	0.3333	0.6667	0.5000	3.72	3Pr(1)+6Co(1)
B(2)	$4h_2$	0.3333	0.6667	0.1157(17)	1.48	3Pr(3)+3Co(3)+3Co(4)

$Z=1$ $a=5.1264(4)$ Å $c=16.5602(6)$ Å

$R_p=9.6\%$ $R_{wp}=12.3$ $R_F=5.9\%$, $R_{\exp}=6.1\%$, $\chi^2=2.0$

C. Saturation magnetization and magnetic moments

Figure 4 shows the magnetization curve at 5 K of a free powder $Pr_5Co_{19}B_6$ sample measured in the SQUID. A saturation moment of $23.7\mu_B$/f.u. was derived by fitting the experimental data of $M(H)$ versus H using the law of approach to saturation. For $Pr_5Co_{19}B_6$ in which Pr is a light R element ($\mathbf{J}=\mathbf{L}-\mathbf{S}$), this implies that the total R moment ($g\mathbf{J}\mu_B$) is coupled parallel to the Co moments. Thus the magnetic moment of $Pr_5Co_{19}B_6$, μ_s, can be expressed as

$$\mu_s = 5\langle\mu_{\mathrm{Pr}}\rangle + 19\langle\mu_{\mathrm{Co}}\rangle, \tag{4}$$

$\langle\mu_{\mathrm{Pr}}\rangle$ and $\langle\mu_{\mathrm{Co}}\rangle$ are the average moments of Pr and Co, respectively. Reliable values of the saturation moment of Co may be obtained for Gd (s state) or Y (nonmagnetic) compounds. In compounds with non-s-state R ions, the Co moment in general cannot be accurately determined because of the unknown reduction of the R moment by crystal-field effects or because of difficulties in saturating the compounds as a result of their high anisotropy. However, it is possible to estimate the moment of the Co sublattice in these systems, if information is available about the R moment. If we assume the average Pr^{3+} moment to be $2.4\mu_B$,[7] an average Co moment $\langle\mu_{\mathrm{Co}}\rangle$ of $0.6\mu_B$ is calculated. It is reasonable to assume that the Co atoms at different sites have different magnetic moments. As can be seen in Fig. 2 and Table I, there are four kinds of Co sites expressed by Co(N) with $N=0$, 1, and 2, where Co(N) means a Co atom which has NB layers just above or just below. Thus the average Co moment of $Pr_5Co_{19}B_6$ is expressed by

TABLE II. Selected atomic distances (Å) in $Pr_5Co_{19}B_6$.

Pr(1)	−2Pr(2)	3.39	Co(2)	−3Pr(2)	2.96
	−12Co(1)	2.93		−3Co(1)	2.49
	−6B(1)	2.96		−3Co(3)	2.48
Pr(2)	−Pr(1)	3.39	Co(3)	−2Pr(2)	3.25
	−Pr(3)	3.31		−2Pr(3)	2.88
	−6Co(1)	3.24		−2Co(2)	2.48
	−6Co(2)	2.96		−4Co(3)	2.56
	−6Co(3)	3.25		−2B(2)	1.77
Pr(3)	−Pr(2)	3.31	Co(4)	−4Pr(3)	3.01
	−Pr(3)	3.16		−4Co(4)	2.56
	−6Co(3)	2.88		−4B(2)	2.42
	−6Co(4)	3.01	B(1)	−3Pr(1)	2.96
	−6B(2)	2.98		−6Co(1)	2.04
Co(1)	−2Pr(1)	2.93	B(2)	−3Pr(3)	2.98
	−2Pr(2)	3.24		−3Co(3)	1.77
	−4Co(1)	2.56		−3Co(4)	2.42
	−2Co(2)	2.49			
	−2B(1)	2.04			

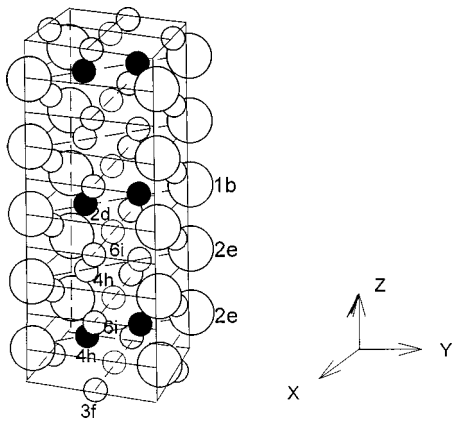

FIG. 2. Crystal structure of $Pr_5Co_{19}B_6$. The large open circles represent Pr, the small open circles Co, and the filled ones B.

$$\langle \mu_{Co} \rangle = [4\langle \mu_{Co(0)} \rangle + 6\langle \mu_{Co(1)} \rangle + 6\langle \mu_{Co(1)} \rangle + 3\langle \mu_{Co(2)} \rangle]/19, \tag{5}$$

where $\mu_{Co(N)}$ represents the magnetic moment of a Co(N) atom. The Co(2) atom at the $3f$ position has B layers just above and below and the B valence electrons may be expected to fill the Co(2)-$3d$ bands. Therefore we assume that $\langle \mu_{Co(2)} \rangle$ is zero, as is found in RCo_3B_2 compounds.[23] The nearest-neighbor environment of Co(0) at the $4h_1$ position is unchanged with respect to the corresponding site in $PrCo_5$, so that $\mu_{Co(0)}$ may be assumed to keep the value of $1.3\mu_B$.[24] By inserting the above values for $\mu_{Co(0)}$, $\mu_{Co(2)}$ and the observed value for $\langle \mu_{Co} \rangle$ into Eq. (5), a value of $0.5\mu_B$ is obtained for $\mu_{Co(1)}$. So, $\mu_{Co(0)}$, $\mu_{Co(1)}$, and $\mu_{Co(2)}$ are $1.3\mu_B$, $0.5\mu_B$, and $0\mu_B$, respectively, showing that the introduction of B results in a strong decrease of the Co moment. Band-structure calculations[25] have shown that the *p*-*d* hybridization lowers the density of states at Fermi energy and reduces the $3d$-band splitting when B atoms preferentially substitute into the nearest-neighbor sites of the Pr atoms.

D. Magnetocrystalline anisotropy

Figures 5(a) and (b) shows the room temperature XRD pattern of an unoriented powder sample and a magnetically aligned sample of $Pr_5Co_{19}B_6$, respectively. It can be seen that the pattern of the aligned sample contains the (200) and (110) peaks. This result clearly demonstrates that the easy magnetization direction (EMD) of $Pr_5Co_{19}B_6$ lies in the basal plane. No anomaly is found in the temperature dependence of magnetization (Fig. 3) and ac susceptibility (Fig. 6) curves. These results suggest that the EMD of $Pr_5Co_{19}B_6$ compound does not change from 5 K to room temperature.

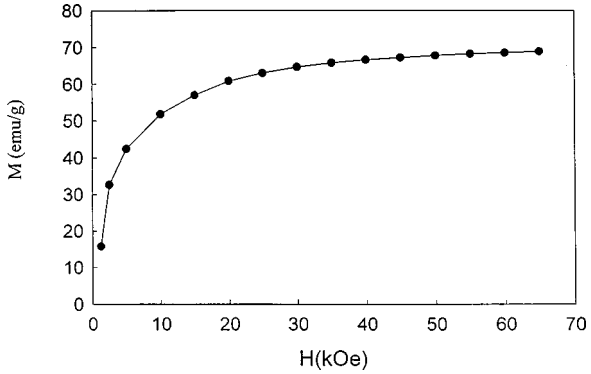

FIG. 4. Field dependence of the magnetization of the free-powder $Pr_5Co_{19}B_6$ at 5 K, measured in a SQUID.

In order to measure the magnetocrystalline anisotropy the sample was prepared by means of the rotation-alignment technique. Rotation-magnetic alignment ensures the HMD of materials which have planar anisotropy to be perpendicular to the applied field direction, i.e., parallel to the cylinder axis of the sample. The rotation-aligned samples were measured in the SQUID at 5 K and in a pulsed magnetic field at 298 K. The results are shown in Figs. 7 and 8, respectively. By linear extrapolation of $\Delta M(=M_{\parallel}-M_{\perp})$ to zero, anisotropy fields H_A of 250 kOe at 5 K and 45 kOe at room temperature are derived. A saturation moment of $11.9\mu_B$/f.u. was derived at 298 K by applying the law of approach to saturation to the experimental $M(H)$ data.

It is well known that the resulting anisotropy in *R*-Co compounds is determined by the sum of the *R* sublattice anisotropy and the Co-sublattice anisotropy. In the case of $R_{m+n}Co_{5m+3n}B_{2n}$ compounds,

$$K_{1,\mathrm{tot}} = (m+n)K_{1,R} + K_{1,\mathrm{Co}}, \tag{6}$$

where $K_{1,R}$ is the contribution of one R^{3+} ion to the anisotropy constant and $K_{1,\mathrm{Co}}$ is the anisotropy constant of the Co

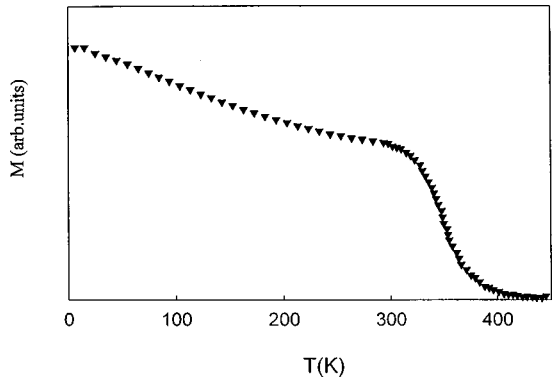

FIG. 3. Thermomagnetic curve for $Pr_5Co_{19}B_6$ in field of about 0.05 T.

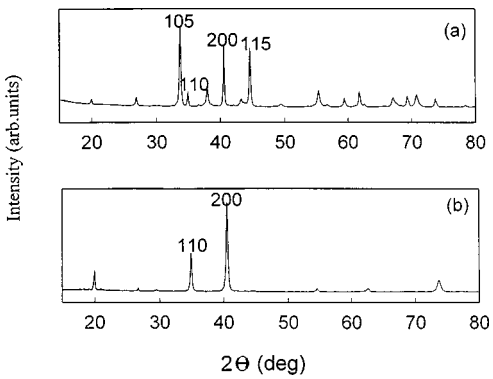

FIG. 5. The XRD patterns of sample $Pr_5Co_{19}B_6$ before (a) and after (b) magnetic alignment.

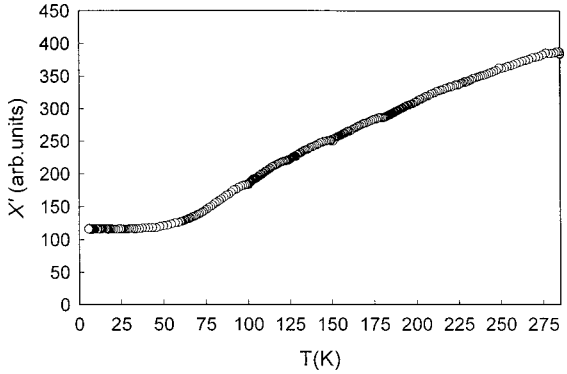

FIG. 6. Temperature dependence of the real component (χ') of the ac susceptibility of bulk $Pr_5Co_{19}B_6$ sample.

sublattice. In first approximation, $K_{1,R}$ can be described as

$$K_{1,R} = -3\alpha_J A_{20}\langle r_{4f}^2\rangle\langle 3J_{R,z}^2 - J_R(J_R+1)\rangle/2, \qquad (7)$$

where α_J is the second-order Stevens coefficient and A_{20} is the second-order crystalline-electric-field (CEF) coefficient. For the $Pr_5Co_{19}B_6$ compounds, the Pr sublattice plays a more important role in determining the EMD at low temperature, and the contribution of Pr sublattice to the anisotropy arises from the coupling between the Pr-ion orbital magnetic moment and the crystalline-electric field. On the basis of a single-ion model,[26] the anisotropy of Pr can be described by the product of α_J and A_{20}. A negative $\alpha_J A_{20}$ exhibits a uniaxial anisotropy. Generally, the second-order CEF coefficient A_{20} is fairly constant in a series of isostructural R compounds in which only the R component is varied. It seems reasonable therefore to use the A_{20} values obtained from the $Gd_{m+n}Co_{5m+3n}B_{2n}$ compounds[6] for analyzing CEF effects in the corresponding Pr compound. ^{155}Gd Mössbauer studies of the series $GdCo_4B$, $Gd_3Co_{11}B_4$, and $Gd_2Co_7B_3$, show that the second-order CEF coefficient A_{20} increases with increasing B substitution. Averaged over the R sites, A_{20} reaches $-1000Ka_0^{-2}$ in the RCo_4B compounds compared with $-700Ka_0^{-2}$ in RCo_5 and $-670Ka_0^{-2}$ in $R_2Fe_{14}B$. The negative sign of A_{20} means that the R ion having a positive second-order Stevens coefficient α_J (Sm^{3+}, Er^{3+}, Tm^{3+}, and Yb^{3+}) shows uniaxial anisotropy, similar to RCo_5 and unlike $R_2Fe_{14}B$. The rare earth Pr has a negative α_J: accordingly, $Pr_5Co_{19}B_6$ has easy-plane anisotropy at low temperature. On the other hand, under the assumptions of the model of individual site contributions to anisotropy (ISA),[4] the Co sites in $Pr_5Co_{19}B_6$ related to the $2c$ site in the RCo_5 structure make large contributions to the magnetocrystalline anisotropy, while the Co sites related to the $3g$ site in the RCo_5 structure make relatively small and reverse contributions. Thus substitution of nonmagnetic B atoms for Co atoms at the sites ($2d$ and $4h_2$) related to the $2c$ site of RCo_5 structure make it possible that $Pr_5Co_{19}B_6$ has its EMD in the basal plane.

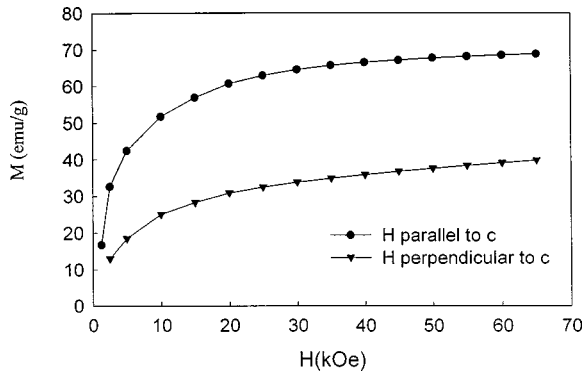

FIG. 7. Magnetization as a function of magnetic field at 5 K for the rotation-alignment $Pr_5Co_{19}B_6$ sample. The upper curve is parallel to the alignment direction and the lower curve is perpendicular to the alignment direction.

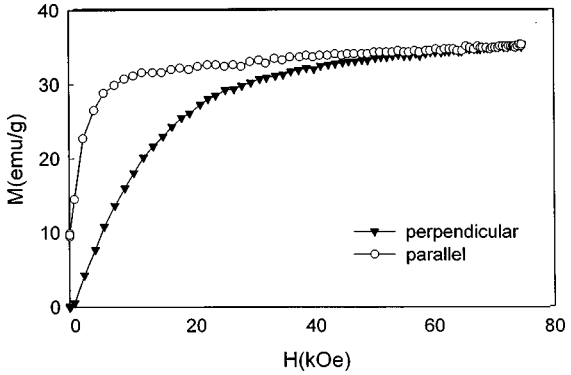

FIG. 8. The magnetic isotherm at room temperature for the rotation alignment $Pr_5Co_{19}B_6$ measured in a pulsed magnetic field, with the external field applied either parallel or perpendicular to the alignment direction of the sample.

IV. CONCLUSIONS

The compound $Pr_5Co_{19}B_6$ has been synthesized. It is a member of the homologous $R_{m+n}Co_{5m+3n}B_{2n}$ series with $m=2$ and $n=3$. Its lattice parameters, unit-cell volume, and density have been determined. The $Pr_5Co_{19}B_6$ compound is ferromagnetic with a Curie temperature of 380 K. Its saturation magnetic moment and anisotropy field at 5 K and 298 K are also obtained. The average Co moment in $Pr_5Co_{19}B_6$ is expressed by $\langle\mu_{Co}\rangle = [4\langle\mu_{Co(0)}\rangle + 6\langle\mu_{Co(1)}\rangle + 6\langle\mu_{Co(1)}\rangle + 3\langle\mu_{Co(2)}\rangle]/19$, where $\mu_{Co(N)}$ denotes the magnetic moment of a Co(N) atom, having N layers of B just above or just below. The introduction of B results in a strong decrease of the Co moment: $\mu_{Co(0)}$, $\mu_{Co(1)}$, and $\mu_{Co(2)}$ are $1.3\mu_B$, $0.5\mu_B$, and $0\mu_B$, respectively. No spin reorientation was detected in the temperature dependence of the magnetization and the temperature dependence of the ac susceptibility. It is quite likely that many intermetallic compounds of the $R_{m+n}Co_{5m+3n}B_{2n}$ family with different m and n are still to be discovered. The compounds of this family may provide interesting opportunities as materials for permanent-magnet application.

ACKNOWLEDGMENTS

This work was supported by the National Natural Science Foundation of China and the State Key Project for Fundamental Research in China. Yi Chen wishes to express his gratitude to J. L. Wang, Y. P. Shen, and S. Y. Fan for their assistance in the magnetic measurements.

[1] M. Sagawa, S. Fujimuro, N. Togawa, H. Yamamoto, and Y. Matsuura, J. Appl. Phys. **55**, 15 (1984).
[2] Yu. B. Kuz'ma and N. S. Bilonizhko, Kristallografiya **18**, 710 (1973) [Sov. Phys. Crystallogr. **18**, 447 (1973)].
[3] H. Ido, K. Sugiyama, H. Hachino, M. Date, S. F. Cheng, and K. Maki, Physica B **177**, 265 (1992).
[4] R. L. Streever, Phys. Rev. B **19**, 2704 (1979).
[5] F. Tasset, Ph.D. thesis, University of Grenoble, 1975.
[6] H. H. Smit, R. C. Thiel, and K. H. J. Buschow, J. Phys. F: Met. Phys. **18**, 295 (1988).
[7] A. T. Pedziwatr, S. Y. Jiang, W. E. Wallace, E. Burzo, and V. Pop, J. Magn. Magn. Mater. **66**, 69 (1987).
[8] R. Tetean and E. Burzo, J. Magn. Magn. Mater. **157/158**, 633 (1996).
[9] T. Ito, H. Asano, H. Ido, and M. Yamada, J. Appl. Phys. **79**, 5507 (1996).
[10] A. E. Nadia and H. H. Stadelmaier, Z. Metallkd. **74**, 86 (1983).
[11] M. Q. Huang, B. M. Ma, L. Y. Zhang, W. E. Wallace, and S. G. Sankar, J. Appl. Phys. **67**, 4981 (1990).
[12] M. Q. Huang, B. M. Ma, S. F. Cheng, and W. E. Wallace, J. Appl. Phys. **69**, 5599 (1991).
[13] H. Ido, H. Ogata, and K. Maki, J. Appl. Phys. **73**, 6269 (1993).
[14] H. Ido, O. Nashima, T. Takahashi, K. Oda, and K. Sugiyama, J. Appl. Phys. **76**, 6165 (1994).
[15] Y. Chen, Q. L. Liu, J. K. Liang, X. L. Chen, B. G. Shen, and F. Huang, Appl. Phys. Lett. **74**, 856 (1999).
[16] Y. Chen, J. K. Liang, X. L. Chen, Q. L. Liu, B. G. Shen, and Y. P. Shen, J. Phys.: Condens. Matter **11**, 8251 (1999).
[17] E. Parthe, B. Chabot, and K. Cenzual, *Gmelin Handbook of Inorganic and Organometallic Chemistry* (Springer, Berlin,1993), Vol. 1, p. 151; Yu. B. Kuz'ma and N. S. Bilonizhko, Kristallografiya **18**, 710 (1973) [Sov. Phys. Crystallogr. **18**, 447 (1974)].
[18] P. E. Werner, Z. Kristallogr. **120**, 375 (1964).
[19] P. E. Werner, J. Appl. Crystallogr. **9**, 216 (1976).
[20] H. M. Rietveld, Acta Crystallogr. **229**, 151 (1967).
[21] H. M. Rietveld, J. Appl. Crystallogr. **2**, 65 (1969).
[22] R. Y. Young, A. Sakthirel, T. S. Moss, and C. O. Paiva-Santos, J. Appl. Crystallogr. **28**, 366 (1995).
[23] H. Ido, M. Nanjo, and H. Yamada, J. Appl. Phys. **75**, 7140 (1994).
[24] W. A. J. J. Velge and K. H. J. Buschow, J. Appl. Phys. **39**, 1717 (1968).
[25] M. Aoki and H. Yamada, Physica B **177**, 259 (1992).
[26] K. H. J. Buschow, Rep. Prog. Phys. **54**, 1123 (1991).